Theoretical studies of the CO_2–N_2O van der Waals complex: Ab initio potential energy surface, intermolecular vibrations, and rotational transition frequencies

Limin Zheng, Soo-Ying Lee, Yunpeng Lu, and Minghui Yang

Citation: The Journal of Chemical Physics **138**, 044302 (2013); doi: 10.1063/1.4776183
View online: http://dx.doi.org/10.1063/1.4776183
View Table of Contents: http://aip.scitation.org/toc/jcp/138/4
Published by the American Institute of Physics

Theoretical studies of the CO_2–N_2O van der Waals complex: *Ab initio* potential energy surface, intermolecular vibrations, and rotational transition frequencies

Limin Zheng,[1] Soo-Ying Lee,[2] Yunpeng Lu,[2,a)] and Minghui Yang[1,a)]
[1]*Key Laboratory of Magnetic Resonance in Biological Systems, State Key Laboratory of Magnetic Resonance and Atomic and Molecular Physics, Wuhan Centre for Magnetic Resonance, Wuhan Institute of Physics and Mathematics, Chinese Academy of Sciences, Wuhan 430071, People's Republic of China*
[2]*Division of Chemistry & Biological Chemistry, School of Physical & Mathematical Sciences, Nanyang Technological University, 21 Nanyang Link, Singapore 637371*

(Received 17 November 2012; accepted 2 January 2013; published online 23 January 2013)

Theoretical studies of the potential energy surface and bound states were performed for the CO_2–N_2O van der Waals complex. A four-dimensional intermolecular potential energy surface (PES) was constructed from 11 466 *ab initio* data points which were calculated at the coupled-cluster single double (triple) level with aug-cc-pVTZ basis set supplemented with bond functions. Three co-planar local minima were found on this surface. They correspond to two equivalent isomers with a slipped parallel structure in which the O atom in N_2O is near the C atom in CO_2 and a T-shaped isomer in which the terminal N atom in N_2O is closest to the C atom in CO_2. The two slipped parallel isomers are energetically more stable than the T-shaped isomer by 178 cm^{-1}. Four fundamental vibrational excited states for the slipped parallel isomers and two fundamental vibrational excited states (torsion and disrotation) for the T-shaped isomer were assigned via bound states calculations based on this PES. The theoretical vibrational frequencies are in good agreement with the available experimental values for the slipped parallel isomers. Rotational excitations (J = 0–6) for the ground vibrational state of the slipped parallel structure were calculated and the accuracy of the PES in the vicinity of minima is validated by the good agreement between the theoretical and experimental transition frequencies and spectroscopic parameters. © *2013 American Institute of Physics*. [http://dx.doi.org/10.1063/1.4776183]

I. INTRODUCTION

Studies on weakly bound clusters or complexes have witnessed significant progress[1] through the remarkable development in high resolution spectroscopic techniques using supersonic expansion and laser, as well as greater availability of high-level *ab initio* calculations in a large scale parallel computing environment. The synergistic interaction between theory and experiment in this field has greatly enhanced our understanding of molecular interactions or intermolecular potential energy, which is responsible for many physical and chemical phenomena including inelastic energy transfer, photo-fragmentation dynamics, and transitions between gas and condensed phases. In principle, if highly accurate intermolecular potential energy surface (PES) is available, the calculations of macroscopic properties in condensed phase can be performed.

CO_2 and N_2O are two molecules at the top of the list of greenhouse gases.[2] It is well known that CO_2 contributes significantly to global warming.[3] Although the concentration of carbon dioxide in the atmosphere is only 0.0034%, its contribution to the overall greenhouse effect is close to 50%.[4] Meanwhile, as an air pollutant, one molecule of N_2O has ~300 times the greenhouse warming potential of one molecule of CO_2.[2] Moreover, N_2O is a precursor for the production of nitrous oxides NO_x which play important roles in the formation of stratospheric ozone.[5,6] Therefore, understanding the physical and chemical properties of these greenhouse molecules and their intermolecular interactions are valuable in the atmospheric and environmental sciences and in industry.

In the past few decades, the van der Waals (vdW) complexes consisting of "CO_2 family" molecules, i.e., CO_2, N_2O, and OCS, have been the subject of extensive experimental and theoretical studies, especially for their dimers[7–30] and trimers.[31–34] Because there is no permanent dipole moment in CO_2, or very small permanent dipole moment in N_2O and OCS, the "driving" force in the formation of these dimers and trimers has been mainly attributed to quadrupole-quadrupole interaction. Recently, some progress have been made in experimental observations of new structures for these complexes, including polar isomers of N_2O[8] and OCS dimers,[14] two distinct structures of OCS–CO_2 complex,[20] and a planar cyclic isomer of CO_2 trimer.[32] Interesting questions, such as the relative stability of the isomers and the interconversion mechanism between these isomers, have been

a)Authors to whom correspondence should be addressed. Electronic addresses: yplu@ntu.edu.sg and yangmh@wipm.ac.cn.

investigated with *ab initio* calculations.[18,21,22,26–30] In particular, potential energy surfaces for CO_2 dimer have been constructed with SAPT method[21] or at MP2 level.[22] Carrington and co-workers have reported the potential energy surface and rovibrational spectrum calculations for N_2O dimer and OCS dimer, respectively.[35,36] A theoretical study of the intermolecular PES and the bound state calculations for the N_2O dimer has also been performed by us.[37] Three co-planar local minima were found on the potential energy surface. They correspond to a nonpolar isomer with slipped-antiparallel planar structure and two equivalent polar isomers with slipped-parallel planar structures. The accuracy of the PES was validated by the good agreement between theoretical and experimental results for the transition frequencies and spectroscopic parameters.

From the study of $(CO_2)_2$ and $(N_2O)_2$ dimers, a planar slipped parallel structure for the heterogeneous CO_2–N_2O complex with two possibilities can be hypothesized: Structure I with the O atom in N_2O closest to the C atom in CO_2, and Structure II with the terminal N atom in N_2O closest to the C atom in CO_2. Dutton *et al.* used high resolution infrared spectroscopy to probe CO_2–N_2O in the CO_2 ν_3 region.[29] Their results were consistent with the slipped parallel structure, but the experiment was unable to determine which structure was observed. Their *ab initio* calculations showed that Structure I corresponds to the global minimum on the potential energy surface. Because of its polarity, the CO_2–N_2O complex can be also studied by means of its rotational spectrum.[38,39] Leung and Marshall had confirmed the validity of Structure I using microwave spectroscopy with isotopic substitution.[39] In 2001, Sordo and co-workers carried out high level *ab initio* prediction of the CO_2–N_2O complex, and concluded that Structure I is the most stable structure.[40] Recently, Moazzen-Ahmadi and co-workers have studied the infrared spectrum of CO_2–N_2O in the regions of the ν_1 and ν_3 fundamentals of N_2O and the ν_3 fundamental of CO_2, and for the first time, the torsion frequency of CO_2–N_2O was determined experimentally to be 25.8 cm^{-1}.[17]

In this work, an *ab initio* potential energy surface has been constructed to further understand the structure and dynamics of the CO_2–N_2O complex. The accuracy of the PES is assessed by comparison of the rotational transition frequencies and spectral parameters between the theoretical calculation and experimental measurement. The comparison of theoretical and experimental vibrational frequencies only validates the accuracy of PES in the vicinity of van der Waals wells which is important to the bound state calculations. We believe that this PES will be useful for the detailed analysis of experimental spectra, as well as the prediction of the structures for the larger size complexes of "CO_2 family" molecules, if more theoretical calculations are performed to validate the accuracy of PES in its asymptotic region. This paper is organized as follows: the computational details for the *ab initio* PES and bound state calculations are described in Sec. II. The results, including the PES, bound state energy levels, intermolecular vibrational fundamental frequencies, and rotational transition frequencies are presented in Sec. III. Finally, we conclude in Sec. IV.

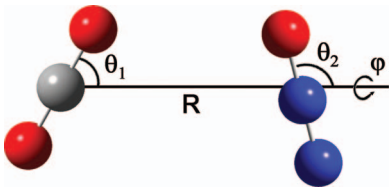

FIG. 1. Jacobi coordinates for CO_2–N_2O van der Waals complex.

II. COMPUTATIONAL DETAILS

A. *Ab initio* calculations of intermolecular potential energy

The CO_2 and N_2O monomers are assumed to be in their ground vibrational state and are approximated as linear rigid rotors with C–O, N–N, and N–O bond lengths fixed at their average values of 1.1615 Å,[41] 1.1273 Å, and 1.1851 Å,[42] respectively. The intermolecular potential energy surface of CO_2–N_2O complex can be described by four Jacobi coordinates (R, θ_1, θ_2, φ) as shown in Fig. 1. R is the vector connecting the centers of mass of the two molecules. The molecular axis of the CO_2 molecule is denoted by vectors r_1 pointing from one end O-atom to the other O-atom, and that of the N_2O molecule is vector r_2 pointing from the N-atom to the O-atom, the angles θ_1 and θ_2 are the enclosed angles of R-r_1 and R-r_2, respectively. The dihedral angle φ is the torsional angle used to describe the out-of-plane vibration.

The *ab initio* potential energy grid was chosen as follows: The radial grid has 18 points ranging from 2.0 Å to 9.0 Å along the R coordinate at the values of 2.00, 2.50, 2.75, 3.00, 3.25, 3.50, 3.75, 4.00, 4.25, 4.50, 4.75, 5.00, 5.50, 6.00, 6.50, 7.00, 8.00, and 9.00 Å, respectively. The angle θ_1 varies from 0° to 180° in steps of 15°, θ_2 varies from 0° to 180° in steps of 15°, and φ varies from 0° to 360° in steps of 30°. Taking account of the symmetry, 11 466 symmetry-unique geometries were finally selected, which covered the short-range repulsive region, the vdW well, and the long-range attractive part of the PES. The intermolecular PES was constructed with an interpolation scheme that was employed in our previous study, and the details can be found in Ref. 37.

The intermolecular potential energy for each geometry was calculated using the supermolecular method at the level of single and double excitation coupled-cluster method with a non-iterative perturbation treatment of triple excitations [CCSD(T)].[43] Based on our previous experience with the N_2O dimer intermolecular potential energy surface, the aug-cc-pVTZ basis set of Woon and Dunning[44] was used in the current work. The bond functions (3*s*3*p*2*d*1*f*) (for 3*s* and 3*p*, a = 0.9, 0.3, 0.1; for 2*d*, a = 0.6, 0.2; for 1*f*, a = 0.3)[45] were also used at the midpoint of the intermolecular distance R. This set of bond functions has been extensively used in the calculations of intermolecular interactions of vdW complexes, such as N_2O–N_2O,[37] CO–CO,[46] Ar–N_2,[47] and H_2–CO_2.[48] The full counterpoise procedure of Boys and Bernardi[49] was employed to correct the basis set superposition error. All the calculations were carried out using the MOLPRO 2006 software package.[50]

B. Bound state calculations

Within the rigid rotor approximation for the monomers, the Hamiltonian of the CO_2–N_2O complex in Jacobi coordinates can be written as[51–53]

$$\hat{H} = -\frac{1}{2\mu}\frac{\partial^2}{\partial R^2} + \frac{1}{2\mu R^2}(\hat{J} - \hat{j}_{12})^2 + B_{CO_2}\hat{j}_1^2 + B_{N_2O}\hat{j}_2^2 + V(R, \theta_1, \theta_2, \varphi). \quad (1)$$

Here, m is the reduced mass of the CO_2–N_2O complex. $\hat{J}$ is the total angular momentum and $\hat{j}_{12} = \hat{j}_1 + \hat{j}_2$, while $\hat{j}_1$ and $\hat{j}_2$ are the angular momenta for CO_2 and N_2O, respectively. B_{CO_2} is the rotational constant of CO_2 with the value of 0.3902 cm^{-1} in its ground vibrational state[54] and B_{N_2O} is the rotational constant of N_2O with the value of 0.4190 cm^{-1} in its ground vibrational state.[55,56]

The wavefunction of the system can be expanded as a linear combination of products of the radial and angular basis functions and written as follows:

$$\Psi = \sum_i \sum_K \sum_{j_1 j_2 j_{12}} c^{iK}_{j_1 j_2 j_{12}} \varphi_i(R)\, Y^{JMK\varepsilon}_{j_1 j_2 j_{12}}, \quad (2)$$

where $\varphi_i(R)$ is a radial basis function describing the intermolecular stretch and is represented by sine functions in this work. ε is the index of the space-inverse parity of the system and $Y^{JMK\varepsilon}_{j_1 j_2 j_{12}}$ is the total symmetry-adapted angular basis function, which has the following explicit form:

$$Y^{JMK\varepsilon}_{j_1 j_2 j_{12}} = \frac{1}{\sqrt{2(1+\delta_{K0})}} \times \left[D^{*J}_{MK} Y^{j_{12}K}_{j_1 j_2} + \varepsilon (-1)^{J+j_1+j_2+j_{12}} D^{*J}_{M-K} Y^{j_{12}-K}_{j_1 j_2} \right]. \quad (3)$$

The total angular basis function is expressed in the body-fixed frame, where D^J_{MK} is a Wigner rotation matrix to describe the overall rotation of the dimer. $Y^{j_{12}K}_{j_1 j_2}$ has the following explicit form:

$$Y^{j_{12}K}_{j_1 j_2}(\theta_1, \theta_2, \varphi) = \sum_m \langle j_1 m_1 j_2 K - m_1 \mid j_{12} K \rangle \times y_{j_1 m_1}(\theta_1, \varphi) \times y_{j_2 K - m_1}(\theta_2, 0), \quad (4)$$

where $\langle j_1 m_1 j_2 K - m_1 \mid j_{12} K \rangle$ is a Clebsch-Gordan coefficient and y_{jm} is a spherical function describing the rotations of the two monomers.

The bound state calculation program is message passing interface (MPI) parallelized and the PARPACK software package was applied to solve for the eigenvalues and eigenfunctions of the bound states.[57] The details of bound state calculation method have been described in our previous works.[37,53] Because of the symmetry of the CO_2 molecule, the eigenfunctions of the CO_2–N_2O complex could be labeled with indexes (ε, j_1) and is divided into 4 symmetry blocks: (+1, odd), (+1, even), (−1, odd), (−1, even). Each block can be solved separately. To compare with experimental microwave spectra, the rovibrational bound states of the CO_2–N_2O complex with the total angular momentum up to J = 6 were calculated. To obtain eigenvalues converged to 0.001 cm^{-1}, 80 sine basis functions were used for R in the range from 4.0 bohrs to 12.0 bohrs, and the size of rotational basis functions is controlled by setting $j_{1\max} = j_{2\max} = 40$ and also depends on both the values of J_{tot} and the parity ε.

III. RESULTS AND DISCUSSION

A. *Ab initio* PES

The geometries and energies of the local minima (A, A′, D), three saddle points (B, G, G′), and four special structures (C, C′, E, E′) on this *ab initio* PES are listed in Table I and also presented in Fig. 2. A and A′ are two equivalent global minima with a well depth of −580.973 cm^{-1} at the configuration of R = 3.429 Å, $\theta_1 = 118.15°$, $\theta_2 = 121.53°$, $\varphi = 0.0°$

TABLE I. Important geometries and their corresponding energies on the PES as well as the calculated energies in other works (R in angstrom, angles in degree, and energy in cm^{-1}).

	Structures in this work				Energy			
	R	θ_1	θ_2	φ	This work	HF/6-311G*[a]	MP2/ AVDZ[b]	QCISD(T)/VDZ[c]
					Local minima			
A	3.429	118.15	121.53	0.0	−580.973	−494	−542	−541
A′	3.429	61.85	121.53	180.0	−580.973			
D	4.300	90.0	0.0	Arbitrary	−402.902	−177	−536	−354
					Saddle points			
B	4.107	90.0	180.0	Arbitrary	−367.076	−307	−390	−355
G	3.950	65.50	42.00	0.0	−383.170			
G′	3.950	114.50	42.00	180.0	−383.170			
					Three special structures			
C	4.140	180.0	90.0	Arbitrary	−410.079	−261		
E	3.708	50.06	65.0	Arbitrary	−397.813	−155	−549	−314
E′	3.708	129.94	65.0	Arbitrary	−397.813			
F	4.140	0.0	90..0	Arbitrary	−410.079			

[a]From Ref. 29.
[b]From Ref. 40. Structure C is proven not to be a minimum when electronic correlation is taken into account in this work.
[c]From Ref. 40.

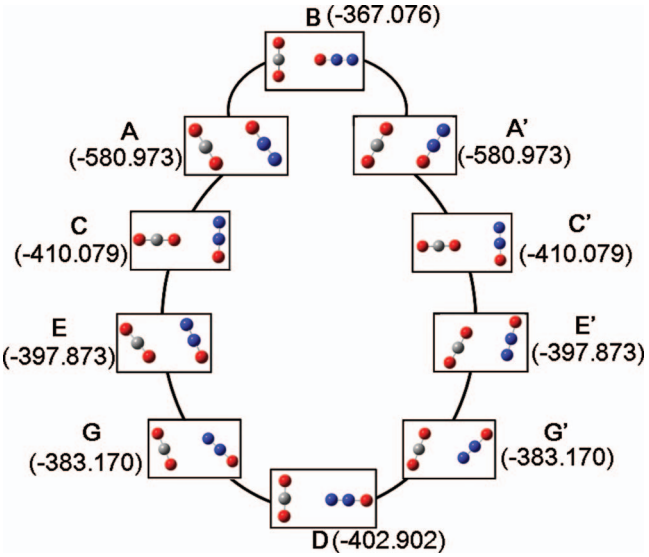

FIG. 2. The pathways connecting the three stable isomers.

and R = 3.429 Å, $\theta_1 = 61.85°$, $\theta_2 = 121.53°$, $\varphi = 180.0°$, respectively, as shown in Fig. 3(a). From Fig. 1 we can see that these two global minima correspond to the planar slipped parallel structures with O in N_2O closest to the C in CO_2, which has been observed in the experiment.[38] D is a local minimum with a well depth of -402.902 cm^{-1} at the configuration of R = 4.3 Å, $\theta_1 = 90.0°$, $\theta_2 = 0.0°$, φ = arbitrary, corresponding to a T-shaped isomer with the terminal N atom in N_2O closest to the C in CO_2. It should be noted that the T-shaped isomer has not been observed in experiment so far. The two equivalent isomers, A and A′, with slipped parallel structures are energetically more stable than the T-shaped isomer by

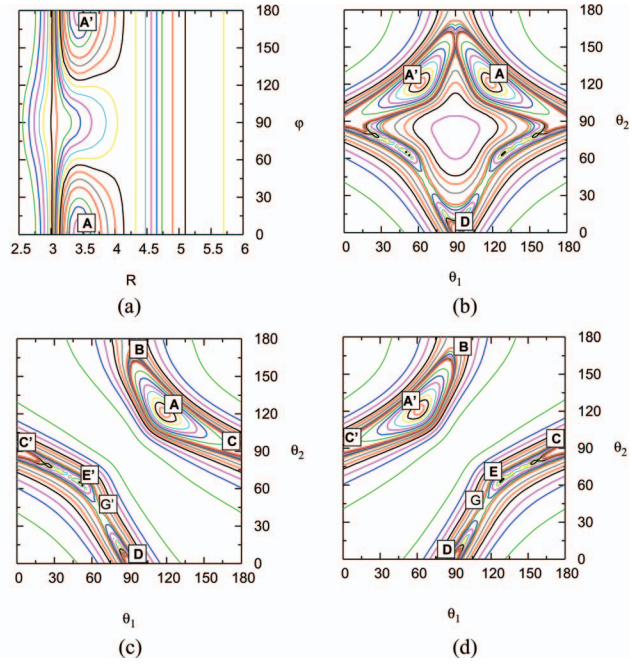

FIG. 3. Contour plots of PES produced by looping over other two coordinates. *R* in angstrom and θ_1, θ_2, and φ in degree. (a) *R*-φ contour plot; (b) θ_1-θ_2 contour plot; (c) θ_1-θ_2 contour plot with $\varphi = 0°$; (d) θ_1-θ_2 contour plot with $\varphi = 180°$.

178.071 cm^{-1}. The locations of A, A′, and D are shown in Fig. 3(b).

After careful analysis of the PES, these local minima are found to be connected via two in-plane minimum energy pathways. These pathways could be characterized by three T-shaped structures (B, C, C′) and four special structures (E and E′, G and G′) (see Fig. 2). These two equivalent global minima (A and A′) could be connected by the two pathways (B pathway and D pathway). The first pathway A-B-A′ (denoted as B pathway) passes through the saddle point B with a barrier height of 213.897 cm^{-1}. The other long pathway A-C-E-G-D-G′-E′-C′-A′ (denoted as D pathway) passes through the local minimum D and two equivalent saddle points G and G′ with a barrier height of 197.803 cm^{-1} (Figs. 2–3(d)). Two equivalent structures E and E′ correspond to two local minima on this potential energy surface with an energy of -397.813 cm^{-1} and very small barrier of about 2 cm^{-1} with respect to the C and C′ structure, respectively. Although the barrier height of D pathway is slightly lower (16 cm^{-1}) than that of B pathway, its distance is much longer than that of B pathway, indicating that the B pathway could be more easily, than the D pathway, connecting A and A′. Moreover, it can be seen from Figs. 2 and 3 that the D pathway connects the A and D (A′ and D) structures through the saddle point G (G′) with a small barrier height of 19.732 cm^{-1}, suggesting the difficulty of the experimental observation of the T-shaped isomer (D structure).

Five structures (A, B, C, D, E) have been discussed in two previous theoretical studies[29,40] and their results are also listed in Table I for comparison. From Table I, we can see that structure A is the most stable with the lowest energy in all studies. The order of the relative energies for the other four structures (B, C, D, E) depends on the computational level. The order of stability for the five structures on this CCSD(T) PES is A > C > D > E > B.

For comparison, the structures and energies of related complexes (CO_2–N_2O, N_2O–N_2O, OCS–OCS, and CO_2–CO_2) are listed in Table II. From Table II, we can see that all four complexes have two planar stable isomers. For both N_2O–N_2O and OCS–OCS complexes, the nonpolar isomer is energetically more stable (162.202 cm^{-1} for N_2O–N_2O and

TABLE II. Comparison of the structures (R in Angstrom, angle in degree) and energies (in cm^{-1}) for some complexes consisting of the CO_2 family of molecules (CO_2, N_2O, and OCS).

Complex	Isomer	*R*	θ_1	θ_2	φ	E
CO_2–N_2O[a]	Parallel slipped	3.429	118.15	121.53	0.0	−580.973
	T-shaped	4.300	90.00	0.00	Arbitrary	−402.902
N_2O–N_2O[b]	Nonpolar	3.379	60.8	119.2	180.0	−627.518
	Polar	3.535	116.1	123.7	0.0	−465.316
OCS-OCS[c]	Nonpolar	3.598	86.880	93.119	180.0	−600.36
	Polar	3.840	75.258	56.575	0.0	−544.37
CO_2–CO_2[d]	Parallel slipped	3.470	59.8	59.8	0.0	−694.6
	T-shaped	4.10	90.0	0.0	Arbitrary	−592.6

[a]This work.
[b]From Ref. 37.
[c]From Ref. 36.
[d]From Ref. 22.

55.99 cm^{-1} for OCS–OCS) than the polar isomer. For both CO_2–N_2O and CO_2–CO_2 complexes, the parallel slipped isomer is energetically more stable (178.071 cm^{-1} for CO_2–N_2O and 102.0 cm^{-1} for CO_2–CO_2) than the T-shaped isomer. The intermolecular distance of the more stable isomer is slightly shorter than that of the less stable one, indicating that the shorter intermolecular distance could result in the stronger vdW interaction.

B. Intermolecular vibrational states

Because of the deep well on this PES and the heavy masses of N_2O and CO_2 monomers, the number of bound states on this PES is numerous. Our initial effort is to obtain the vibrational excited states corresponding to four fundamental intermolecular vibrational modes for both the slipped parallel and T-shaped isomers. These vibrational states can be assigned by analyzing the reduced-dimensional contour plots of their wavefunctions. Similar to the N_2O–N_2O dimer,[37] the vibrational states are labeled with four intermolecular vibrational modes (n_{tor}, n_{dis}, n_r, n_{co}). They are the out-of-plane torsion, in-plane disrotation (or "in-plane geared bending"), dissociation (or vdW stretch), and in-plane conrotation (or in-plane antigeared bending) modes, respectively. Four fundamental vibrational excited states of the slipped parallel isomer are all assigned. While for the T-shaped isomer, only the torsion and disrotation vibrational excited states could be assigned unambiguously. The other excited states could not be assigned in a satisfactory manner due to the shallow well of the T-shaped minimum and the wavefunction mixing heavily with the wavefunction located in the slipped parallel well. The energy levels of the successfully assigned vibrational states are listed in Table III and the comparison of the fundamental frequencies with the experimental values and *ab initio* calculated values are summarized in Table IV.

Because of the high barrier (213.897 cm^{-1}) between the two equivalent global minima, quantum tunneling could not occur and the ground vibrational states are doubly degenerate (one is the 1st root in the (+1, even) symmetry block and the other is the 1st root in the (+1, odd) symmetry block) with an energy of −469.620 cm^{-1} and a zero point energy of 111.353 cm^{-1}. For the T-shaped isomer, the ground vibrational state corresponds to the 30th root in the (+1, even) block with a bound energy of 328.833 cm^{-1}. The corresponding zero point energy is 74.070 cm^{-1}, indicating a wider potential well for the T-shaped isomer than for the slipped parallel isomers.

The intermolecular vibrational excited states could be identified from their wavefunction plots in DVR by counting the number of nodal points or nodal surfaces. With the help of the contour plots (see Fig. 4), the disrotation and conrotation excited states of the slipped parallel isomer are

TABLE III. The intermolecular vibrational energy levels (in cm^{-1}) and assignments (n_{tor}, n_{dis}, n_r, n_{co}) for both slipped parallel and T-shaped isomers. Only the ground vibrational and torsion states are assigned in this work. Block is labelled by (ε, j_1), where ε is the index of the space-inverse parity of the system and j_1 is the angular momentum for CO_2 monomer.

Assignment	Energy	Frequency	(ε, j_1)	No. in block
Slipped parallel isomer				
(0,0,0,0)	−469.620		(+1, even)	1
(1,0,0,0)	−443.860	25.760	(−1, even)	1
(0,1,0,0)	−437.170	32.450	(+1, even)	2
(0,0,1,0)	−425.009	44.611	(+1, even)	3
(0,0,0,1)	−373.219	96.401	(+1, even)	11
T-shaped isomer				
(0,0,0,0)	−328.832		(+1, even)	30
(1,0,0,0)	−311.190	17.642	(−1, odd)	29
(0,1,0,0)	−320.571	8.261	(+1,odd)	37

TABLE IV. Intermolecular vibrational frequencies (in cm^{-1}) for both slipped parallel and T-shaped isomers.

	HF/6-311G*[a]	MP2/aug-cc-pVTZ[b]	Bound state Calc.	Expt.[c]
Slipped parallel isomer				
Torsion	32.01	27.38	25.760	25.8
Disrotation	29.06	38.58	32.450	
Dissociation	45.59	58.60	44.612	
Conrotation	110.55	108.37	96.401	
T-shaped isomer				
Torsion		17.66	17.642	
Disrotation		8.68	8.261	
Dissociation		64.25		
Conrotation		74.41		

[a]From Ref. 29.
[b]Calculated in this work with G09 Software package.[59]
[c]From Ref. 17.

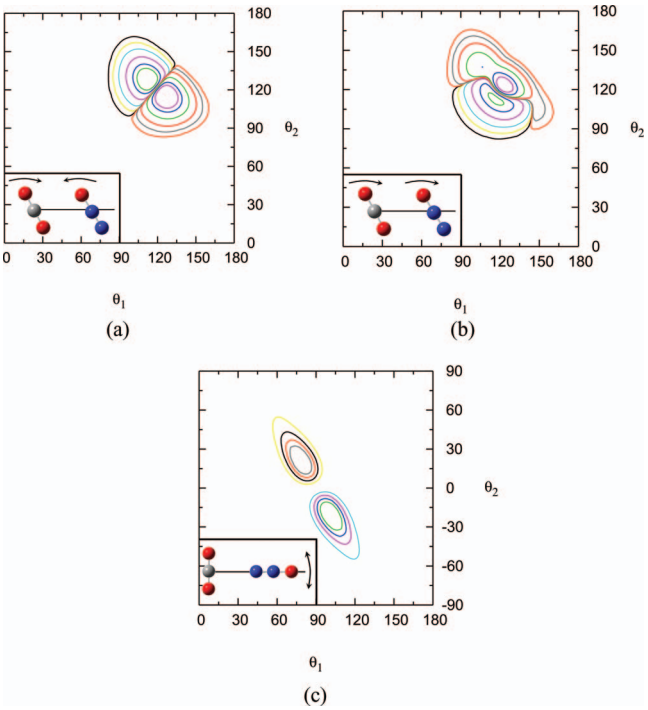

FIG. 4. θ_1-θ_2 contour plots of the wavefunctions and the vibrational modes for the slipped parallel isomer. (a) Disrotation mode for the slipped parallel isomer; (b) Conrotation mode for the slipped parallel isomer; (c) Disrotation mode for the T-shaped isomer.

assigned to be the 2nd root and the 11th root in the (+1, even) symmetry block, respectively. In our previous work,[37] the dynamic information of the N_2O–N_2O polar isomer is analyzed by connecting the orientation of the nodal surface to the classical picture of vibrations. In this work, the same technique is also used to identify the disrotation and conrotation vibrational modes for the slipped parallel isomer. From Fig. 4, one can see that the orientation of the nodal surface is about $+45^\circ$ for disrotation mode and the changes of θ_1 and θ_2 are out-of-phase. For the conrotation mode, the orientation of the nodal surface is about -45°, which corresponds to changes of θ_1 and θ_2 that are in-phase.

The fundamental vibrational frequencies in the bound state calculations are compared with the *ab initio* calculated values in Table IV. The calculated frequencies at the MP2/aug-cc-pVTZ level have the same trend with those obtained from bound state calculations. However, the previous calculated frequencies at the HF/6-311G* level show different order for the torsion and disrotation modes, indicating that to some extent the HF/6-311G* method could not estimate the frequency correctly.[30] Using a harmonic model, the zero point energy (ZPE) is 116.46 cm^{-1} at MP2/aug-cc-pVTZ level and is 99.61 cm^{-1} from fundamental frequencies. Both values are slightly different from the bound state calculated ZPE of 111.353 cm^{-1} and indicated the anharmonic effect is weak for the slipped parallel isomers.

So far, only the torsion vibrational frequency has been experimentally measured with a value of 25.8 cm^{-1} for the slipped parallel isomer of the CO_2–N_2O complex with CO_2 ν_1 or N_2O ν_3 stretch excitations.[17] As the intramolecular vibrational frequencies of CO_2 ν_1 or N_2O ν_3 stretch are significantly larger than the intermolecular torsion vibrational frequency, the measured torsion vibrational frequency could be very close to the ground state torsional frequency and is used to assess various theoretical calculation values. The previous calculated frequency[29] for this mode at HF/6-311G* level is 32.01 cm^{-1} and our MP2/aug-cc-pVTZ calculated value is 27.39 cm^{-1}. The frequency obtained from the bound state calculations is 25.76 cm^{-1} and the deviation is only 0.04 cm^{-1}. The excellent agreement between the theoretical and experimental values shows the ability of this *ab initio* PES to predict the bound states.

Since there are two equivalent structures for the slipped parallel isomer, the quantum tunneling effect is an interesting topic. In this work, the tunneling splittings are almost zero for the ground and four excited states, indicating that the quantum tunneling effects can be neglected for these states. Also, one can see in Fig. 4 that even for the highest conrotation vibrational excited state, its wavefunction has no distribution near the saddle point B. This phenomenon could be explained by the much higher barrier (213.897 cm^{-1}) between the two equivalent isomers.

For the T-shaped isomer (see Table III), only the torsion and disrotation vibrational excited states are assigned to be the 29th root in the (−1, odd) block with an excited energy of 17.642 cm^{-1} and the 37th root in the (+1, odd) symmetry block with an excited energy of 8.261 cm^{-1}, respectively. Because of the small barrier height between the two types of isomers, the wavefunction of other higher excited states diffuses from the T-shaped well to the slipped parallel well and these higher excited states are not assigned successfully in this work. From Table IV, we can see that the calculated frequencies (17.66 cm^{-1} and 8.68 cm^{-1}) of the torsion and disrotation vibrational states at the MP2/aug-cc-pVTZ level agree well with the corresponding bound state calculated values (17.642 cm^{-1} and 8.261 cm^{-1}). The zero point energy from the MP2/aug-cc-pVTZ calculation is 82.50 cm^{-1} which is slightly larger than the corresponding value (74.040 cm^{-1}) obtained from the bound state calculation.

TABLE V. The average structural parameters of the ground vibrational states for both slipped parallel and T-shaped isomers (R in angstrom and angles in degree).

	Slipped parallel isomer			T-shaped isomer
	Expt.[a]	Expt.[b]	This work	This work
$\langle R \rangle$	3.470	3.472	3.498	4.298
$\langle \theta_1 \rangle$	119.9	117.2	118.890	82.316
$\langle \theta_2 \rangle$	119.9	121.9	120.879	14.615

[a]From Ref. 29.
[b]From Ref. 38.

The average structural parameters $\langle R \rangle$, $\langle \theta_1 \rangle$, and $\langle \theta_2 \rangle$ for a vibrational states can be determined from the related wavefunctions using the following formulas:[47,48]

$$\left\langle \frac{1}{R^2} \right\rangle \approx \frac{1}{\langle R^2 \rangle} \quad \text{and} \quad P_2(\cos\langle\theta\rangle) = \langle P_2(\cos\theta)\rangle,$$

where θ denotes angles θ_1 or θ_2. P_2 is the second order Legendre function and $\langle P_2(\cos\theta)\rangle$ is the average value of the Legendre function for the state of interest. The calculated structural parameters of the ground states of the CO_2–N_2O complex for both slipped parallel and T-shaped structures are listed in Table V, as well as the experimental values for the slipped parallel isomer. One can see that the calculated average parameters agree well with the experimental values for the slipped parallel isomers. It is interesting to compare the structural parameters between local minima on PES and the vibrational average values. For both isomers, the intermolecular distances deviate slightly from the local minima on PES, 0.07 Å for the parallel isomer and 0.002 Å for the T-shaped isomer, respectively, reflecting the effects of small amplitude motion and zero point energy. For the T-shaped isomer, the larger deviations of $\langle \theta_1 \rangle$ and $\langle \theta_2 \rangle$ from their equilibrium values can be thought of as an effect of librational motion of the monomers in the complex.

C. Rotational transition frequencies of the slipped parallel isomer

Due to its polarity, rotational spectra for the CO_2–N_2O slipped parallel isomer have been observed previously.[38,39] In 1998, Leung obtained the microwave spectrum of CO_2–N_2O in the 7–19 GHz region using a Fourier transform microwave spectrometer.[38] In that work, 26 rotational transitions, including 11 *a*-type and 15 *b*-type transitions (see Table VII), were identified for the normal isotopomer CO_2–$^{14}N_2O$. In 1999, Leung and Marshall subsequently carried out another microwave study with isotopic substitution to

TABLE VI. Calculated pure rotational energy levels (in cm^{-1}) of the slipped parallel CO_2–N_2O complex.

	$J_{tot} = 0$	(431)	−466.3689
(000)	−469.6206	(441)	−464.6589
		(440)	−464.6589
	$J_{tot} = 1$		
(101)	−469.5155		$J_{tot} = 5$
(111)	−469.2757	(505)	−468.0541
(110)	−469.2663	(515)	−467.8721
		(514)	−467.7321
	$J_{tot} = 2$	(524)	−467.0674
(202)	−469.3057	(523)	−467.0581
(212)	−469.0749	(533)	−465.8427
(211)	−469.0469	(532)	−465.8426
(221)	−468.3274	(542)	−464.1329
(220)	−468.3271	(541)	−464.1329
		(551)	−461.9353
	$J_{tot} = 3$	(550)	−461.9353
(303)	−468.9915		
(313)	−468.7739		$J_{tot} = 6$
(312)	−468.7178	(606)	−467.4329
(322)	−468.0122	(616)	−467.2719
(321)	−468.0108	(615)	−467.0761
(331)	−466.7898	(625)	−466.4383
(330)	−466.7898	(624)	−466.4199
		(634)	−465.2110
	$J_{tot} = 4$	(633)	−465.2106
(404)	−468.5740	(643)	−463.5015
(414)	−468.3729	(642)	−463.5015
(413)	−468.2794	(652)	−461.3040
(423)	−467.5921	(651)	−461.3040
(422)	−467.5881	(661)	−458.6196
(432)	−466.3689	(660)	−458.6196

confirm the validity of Structure I for the slipped parallel isomer.[39] To our best knowledge, the T-shaped isomer has not been successfully observed in experiment so far. In addition, the ground vibrational state energy of the T-shaped isomer (−328.832 cm^{-1}) is much higher than that of the slipped parallel isomer (−469.620 cm^{-1}), indicating a very high cost to calculate the rotational transitions for the T-shaped isomer. Therefore, we limited our calculation to the pure rotational spectra for the slipped parallel isomer in this work.

The rotational energy levels for $J = 0$–6 of the ground vibrational state of the slipped parallel isomer and their assignments are listed in Table VI. The theoretical transition frequencies and their deviations from experimental values are listed in Table VII. We can see that the RMSD between the experimental and calculated values is only 0.006 cm^{-1} and the maximum deviation is 0.014 cm^{-1} with the transition $3_{22} \rightarrow 4_{13}$.

In order to compare the spectroscopic parameters with experimental values directly, the theoretical rotational energy levels are fitted with the same Hamiltonian used in the experiment, a Watson asymmetric rotor expression employing the A-type reduction in the *Ir* representation,[58]

$$H = \frac{1}{2}(B+C)J^2 + \left[A - \frac{1}{2}(B+C)\right]J_a^2 + \frac{1}{2}(B-C)\left(J_b^2 - J_c^2\right) - \Delta_{JK}J_a^2J^2 - \Delta_K J_a^4 - 2\delta_J J^2(J_b - J_c) - \delta_k\left[J_a^2\left(J_b^2 - J_c^2\right) + \left(J_b^2 - J_c^2\right)J_a^2\right].$$

The fitted parameters show excellent agreement with the corresponding experimental values[8] (see Table VIII). In Table VIII, the inertial defect of CO_2–N_2O slipped parallel isomer is also listed. The calculated value is 1.243 amuÅ^2, which is larger than the experimental measurement by 0.459 amuÅ^2. The small positive value of the inertial defect implies that the parallel slipped isomer has the planar structure. The discrepancy can be explained by the fact that the rotational constants are fitted by all the rotational energy levels in this work but fitted by only 26 resolved transitions in experiment.

TABLE VII. Calculated transition frequencies (in cm^{-1}) of the slipped parallel CO_2–N_2O complex. The experimental data are taken from Ref. 38. The numbers in parentheses indicate the residuals between calculated and experimental results.

$J'_{K_{a'}K_{c'}} - J''_{K_{a''}K_{c''}}$	Freq. (Calc. − Expt.)	$J'_{K_{a'}K_{c'}} - J''_{K_{a''}K_{c''}}$	Freq. (Calc. − Expt.)
$1_{10} - 1_{01}$	0.2492(0.0025)	$6_{15} - 6_{06}$	0.3568(−0.0013)
$3_{22} - 4_{13}$	0.2673(0.0147)	$2_{21} - 3_{12}$	0.3904(0.0128)
$2_{11} - 2_{02}$	0.2588(0.0023)	$4_{14} - 3_{13}$	0.4010(−0.0045)
$3_{12} - 3_{03}$	0.2737(0.0017)	$4_{04} - 3_{03}$	0.4175(−0.0049)
$4_{13} - 4_{04}$	0.2945(0.0010)	$4_{23} - 3_{22}$	0.4200(−0.0051)
$3_{13} - 2_{12}$	0.3009(−0.0034)	$2_{20} - 3_{13}$	0.4467(0.0111)
$3_{03} - 2_{02}$	0.3141(−0.0037)	$2_{12} - 1_{01}$	0.4406(0.0005)
$3_{22} - 2_{21}$	0.3152(−0.0038)	$4_{13} - 3_{12}$	0.4383(−0.0057)
$3_{21} - 2_{20}$	0.3162(−0.0039)	$6_{06} - 5_{15}$	0.4391(−0.0114)
$5_{14} - 5_{05}$	0.3219(0.0000)	$5_{05} - 4_{04}$	0.5199(-0.0060)
$5_{05} - 4_{14}$	0.3188(−0.0099)	$5_{24} - 4_{23}$	0.5246(−0.0064)
$3_{12} - 2_{11}$	0.3290(−0.0042)	$3_{13} - 2_{02}$	0.5317(−0.0002)
$1_{11} - 0_{00}$	0.3449(0.0015)	$4_{14} - 3_{03}$	0.6186(−0.0010)
RMSD		0.0062	

TABLE VIII. Comparison of the spectroscopic parameters and the inertial defects for the slipped parallel CO_2–N_2O complex in the ground vibrational state.

Parameter	Expt. [a]	Calc.
A	0.2949845	0.2973726
B	5.7999361×10^{-2}	5.7999693×10^{-2}
C	4.8360363×10^{-2}	4.8360497×10^{-2}
Δj	2.1715020×10^{-7}	1.5996889×10^{-5}
Δk	7.8250787×10^{-6}	1.8734718×10^{-6}
Δjk	$-1.2476963 \times 10^{-6}$	$-2.7785450 \times 10^{-6}$
δj	$-4.5868394 \times 10^{-8}$	1.7745423×10^{-6}
δk	$-2.7685816 \times 10^{-9}$	1.5633674×10^{-7}
Inertial defect	0.784 amu Å^2	1.243 amu Å^2

[a]From Ref. 38.

IV. CONCLUSIONS

In this paper, theoretical studies of the potential energy surface and bound states were performed for the CO_2–N_2O vdW complex. A four-dimensional intermolecular PES was constructed at the CCSD(T) level with aug-cc-pVTZ basis set supplemented with bond functions. Three co-planar local minima were found on this surface. They correspond to two equivalent slipped parallel isomers in which the O atom in N_2O is near the C atom in CO_2 and a T-shaped isomer in which the terminal N atom in N_2O is close to the C atom in CO_2. The dissociation energies of the two kinds of isomers are 580.973 cm^{-1} and 402.902 cm^{-1}, respectively. The slipped parallel isomers are energetically more stable than the T-shaped isomer by 178 cm^{-1}. From the bound state calculations, the ground state energy of the slipped parallel isomers is -469.620 cm^{-1} with a zero point energy of 111.353 cm^{-1}. The corresponding values for the T-shaped isomer are -328.832 cm^{-1} and 74.070 cm^{-1}, respectively.

Four intermolecular fundamental vibrational states for the slipped parallel isomer are assigned from an analysis of their wavefunctions. The calculated torsion vibrational frequency (25.760 cm^{-1}) is in good agreement with the experimental measurement (25.8 cm^{-1}). Because of the much higher barrier (213.897 cm^{-1}) between the two equivalent slipped parallel isomers, the quantum tunneling effects can be neglected in the ground and four excited states, and these bound states are all doubly degenerate.

For the T-shaped isomer, only the torsion and disrotation vibrational states are assigned with calculated frequencies of 17.642 cm^{-1} and 8.261 cm^{-1}, respectively. The other two fundamental excited states are not successfully assigned due to the lower barrier between the slipped parallel and T-shaped isomers. It is interesting to note that it is not the torsion but the disrotation vibrational frequency that is the smallest among the four fundamental frequencies.

Twenty six experimental rotational frequencies are compared with the calculated frequencies. The maximum deviation between the experimental and calculated values is 0.014 cm^{-1} and the RMSD is 0.006 cm^{-1}. The good agreement between theory and experiment showed the high accuracy of this *ab initio* PES in the vicinity of van der Waals wells.

ACKNOWLEDGMENTS

This work was supported by (1) the National Science Foundation of China (Projects Nos. 21221064, 21073229, and 20833007) and (2) the Ministry of Education, Singapore, Grant No. MOE2011-T2-2-087.

[1]See the articles in B. Brutschy and P. Hobza, Chem. Rev. **100**, 3861–4264 (2000).
[2]See http://en.wikipedia.org/wiki/Greenhouse_gas for the introduction of greenhouse gas.
[3]P. H. Abelson, Science **289**, 1293 (2000); D. Bakker and A. Watson, Nature (London) **410**, 765 (2001).
[4]I. M. Mintzer, Annu. Rev. Energy **15**, 513 (1990).
[5]P. J. Crutzen, Angew. Chem., Int. Ed. Engl. **35**, 1758 (1996).
[6]M. S. Ngri and W. Jager, J. Mol. Spectrosc. **192**, 320 (1998).
[7]A. Hecker, I. Scheelez, and M. Havenith, Phys. Chem. Chem. Phys. **5**, 2333 (2003).
[8]M. Dehghany, M. Afshari, Z. Abusara, N. Moazzen-Ahmadi, and A. R. W. McKellar, J. Chem. Phys. **126**, 164310 (2007).
[9]M. Dehghany, M. Afshari, N. Moazzen-Ahmadi, and A. R. W. McKellar, Phys. Chem. Chem. Phys. **10**, 1658 (2008).
[10]M. Dehghany, M. Afshari, R. I. Thompson, N. Moazzen-Ahmadi, and A. R. W. McKellar, J. Mol. Spectrosc. **252**, 1 (2008).
[11]N. R. Walker, A. J. Minei, S. E. Novick, and A. C. Legon, J. Mol. Spectrosc. **251**, 153 (2008).
[12]C. Y. Wang, A. W. Liu, V. I. Perevalov, S. A. Tashkun, K. F. Song, and S. M. Hu, J. Mol. Spectrosc. **257**, 94 (2009).
[13]M. Dehghany, M. Afshari, Z. Abusara, and N. Moazzen-Ahmadi, Phys. Chem. Chem. Phys. **11**, 7585 (2009).
[14]M. Afshari, M. Dehghany, Z. Abusara, N. Moazzen-Ahmadi, and A. R. W. McKellar, J. Chem. Phys. **126**, 071102 (2007).
[15]M. Afshari, M. Dehghany, Z. Abusara, N. Moazzen-Ahmadi, and A. R. W. McKellar, Chem. Phys. Lett. **442**, 212 (2007).
[16]M. Afshari, Z. Abusara, N. Dehghany, N. Moazzen-Ahmadi, and A. R. W. McKellar, Chem. Phys. Lett. **437**, 23 (2007).
[17]M. Afshari, M. Dehghany, N. Moazzen-Ahmadi, and A. R. W. Mckellar, J. Chem. Phys. **129**, 074314 (2008).
[18]G. M. Berner, A. L. L. East, M. Afshari, M. Dehghany, N. Moazzen-Ahmadi, and A. R. W. McKellar, J. Chem. Phys. **130**, 164305 (2009).
[19]G. Sedo and J. V. Wijngaarden, J. Chem. Phys. **131**, 044303 (2009).
[20]M. Dehghany, J. Norooz Oliaee, M. Afshari, N. Moazzen-Ahmadi, and A. R. W. McKellar, J. Chem. Phys. **130**, 224310 (2009).
[21]R. Bukowski, J. Sadlej, B. Jeziorski, P. Jankowski, K. Szalewic, S. A. Kucharskid, H. L. Williams, and B. M. Rice, J. Chem. Phys. **110**, 3785 (1999).
[22]S. Bock, E. Bich, and E. Vogel, Chem. Phys. **257**, 147 (2000).
[23]Z. S. Huang and R. E. Miller, J. Chem. Phys. **89**(9), 5408 (1988).
[24]H. B. Qian, W. A. Herrebout, and B. J. Howard, Mol. Phys. **91**(4), 689 (1997).
[25]Y. Ohshima, Y. Matsumoto, M. Takami, and K. Kuchitsu, Chem. Phys. Lett. **152**, 294 (1988).
[26]J. Sadlej and M. Sicinska, J. Mol. Struct.: THEOCHEM **204**, 1 (1990).
[27]K. Mogi, T. Komine, and K. Hirao, J. Chem. Phys. **95**, 8999 (1991).
[28]L. M. Nxumalo, T. A. Ford, and A. J. Cox, J. Mol. Struct.: THEOCHEM **307**, 153 (1994).
[29]C. Dutton, A. Sazonov, and R. A. Beaudet, J. Phys. Chem. A **100**, 17772 (1996).
[30]H. Valdés and J. A. Sordo, J. Phys. Chem. A **108**, 2062 (2004).
[31]H. Valdés and J. A. Sordo, J. Phys. Chem. A **106**, 3690 (2002).
[32]M. Dehghany, M. Afshari, N. Moazzen-Ahmadi, and A. R. W. McKellar, J. Chem. Phys. **128**, 064308 (2008).
[33]M. Dehghany, M. Afshari, N. Moazzen-Ahmadi, and A. R. W. McKellar, J. Chem. Phys. **130**, 044303 (2009).
[34]S. Tsuzuki, W. Klopper, and H. P. Lüthi, J. Chem. Phys. **111**, 3846 (1999).
[35]R. Dawes, X.-G. Wang, A. W. Jasper, and T. Carrington, J. Chem. Phys. **133**, 134304 (2010).
[36]J. Brown, X.-G. Wang, R. Dawes, and T. Carrington, J. Chem. Phys. **136**, 134306 (2012).
[37]L. M. Zheng, Y. P. Lu, S.-Y. Lee, H. Fu, and M. H. Yang, J. Chem. Phys. **134**, 054311 (2011).
[38]H. O. Leung, J. Chem. Phys. **108**, 3955 (1998).
[39]M. D. Marshall and H. O. Leung, J. Mol. Spectrosc. **196**, 149 (1999).

[40]H. Valdes, V. M. Rayon, and J. A. Sordo, Int. J. Quantum Chem. **84**, 78 (2001).
[41]G. S. Yan, M. H. Yang, and D. Q. Xie, J. Chem. Phys. **109**, 10284 (1998).
[42]J. L. Teffo and A. Chedin, J. Mol. Spectrosc. **135**, 389 (1989).
[43]C. Hampel, K. Peterson, and H. J. Werner, Chem. Phys. Lett. **190**, 1 (1992).
[44]D. E. Woon and T. H. Dunning, J. Chem. Phys. **98**, 1358 (1993).
[45]T. B. Pedersen, B. Fernandez, H. Koch, and J. Makarewicz, J. Chem. Phys. **115**, 8431 (2001).
[46]G. W. M. Vissers, A. Heßelmann, G. Jansen, P. E. S. Wormer, and A. van der Avoird, J. Chem. Phys. **122**, 054306 (2005).
[47]J. Zhu, Y.-P. Lu, X.-R. Chen, and Y. Cheng, Eur. Phys. J. D **33**, 43 (2005).
[48]H. Ran, Y. Z. Zhou, and D. Q. Xie, J. Chem. Phys. **126**, 204304 (2007).
[49]S. F. Boys and F. Bernardi, Mol. Phys. **19**, 553 (1970).
[50]H. J. Werner, P. J. Knowles, R. Lindh, F. R. Manby, M. Schütz *et al.*, MOLPRO, version 2006.2, a package of *ab initio* programs (2006).
[51]D. C. Clary and P. J. Knowles, J. Chem. Phys. **93**, 6334 (1990).
[52]D. H. Zhang, Q. Wu, J. Z. H. Zhang, M. V. Dirke, and Z. Bac, J. Chem. Phys. **102**, 2315 (1995).
[53]L. Wang, M. H. Yang, A. R. W. Mckellar, and D. H. Zhang, Phys. Chem. Chem. Phys. **9**, 131 (2007).
[54]M. Keil and G. A. Parker, J. Chem. Phys. **82**, 1947 (1985).
[55]R. A. Toth, J. Opt. Soc. Am. B **4**, 357 (1987).
[56]Y. Z. Zhou and D. Q. Xie, J. Chem. Phys. **120**, 8575 (2004).
[57]R. Lehoucq, D. C. Sorensen, and C. Yang, ARPACK User's Guide: Solution of Large-Scale Eigenvalue Problems with Implicitly Restarted Arnoldi Methods, SIAM, Philadelphia, PA, 1998 (http://www.caam.rice.edu/software/ARPACK).
[58]M. J. Weida, J. M. Sperhac, D. J. Nesbitt, and J. M. Hutson, J. Chem. Phys. **101**, 8351 (1994).
[59]M. J. Frisch, G. W. Trucks, H. B. Schlegel *et al.*, GAUSSIAN 09, Revision B.01, Gaussian, Inc., Wallingford, CT, 2009.